Supporting information

Composition Dependent Band Structure Parameters and Band-Gap Bowing Effect in Caesium Lead mix Halide system: A Cyclic Voltammetry Investigation.

Authors: Suyog S. Mane, Archisman Sinha, and Santosh K. Haram*

Department of Chemistry, Savitribai Phule Pune University, Pune 411 007, India.

AUTHOR INFORMATION

Corresponding Author

*Email: santosh.haram@unipune.ac.in

S1. Procedures for Drying the Solvents and Supporting Electrolyte:

To eliminate moisture from the solvent i.e. DCM, molecular sieves of pore-size 3A were employed. Additionally, the supporting electrolyte i.e. Tetra Butyl Ammonium Perchlorate (TBAP) was subjected to a drying process by placing it in a vacuum oven and maintaining a temperature of 80 °C for an hour. These procedures were implemented to ensure the removal of any residual moisture or other volatile impurities from both DCM and TBAP.

S2. Detail analysis of XRD pattern:

To measure the crystallite size of $CsPbX_3$ perovskite nanocrystals (PNCs) in their cubic phase, we can employ crystallographic principles and geometric relationships. In the cubic phase, the $CsPbX_3$ perovskite structure adopts a cubic lattice.[42]

1. **Side Length Measurement (a):** The side length (a) of the cubic unit cell can be determined using the formula:

$$a = 2\,r_{X^-} + 2r_{Pb^{2+}}$$

$$a = 2\,(r_{X^-} + r_{Pb^{2+}})$$

Here, r_{X^-} represents the ionic radius of the halide ion (X^-) and $r_{Pb^{2+}}$ represents the ionic radius of the lead ion (Pb^{2+}). By adding the radii of these ions and multiplying by 2, we obtain the length of one side of the cubic unit cell.

2. **Diagonal Length Measurement :** The diagonal length of the cubic unit cell can be calculated using the Pythagorean theorem for a cube:

$$a^2 + a^2 = \left(2\,r_{X^-} + 2r_{Cs^+}\right)^2$$

$$2a^2 = \left(2\,r_{X^-} + 2r_{Cs^+}\right)^2$$

$$\sqrt{2}a = 2(r_{X^-} + r_{Cs^+})$$

$$a = \sqrt{2}(r_{X^-} + r_{Cs^+})$$

Here, r_{Cs^+} represents the ionic radius of the cesium ion (Cs^+). By adding the radii of the halide and cesium ions, and then multiplying by $\sqrt{2}$, we obtain the diagonal length of the cubic unit cell.

Table S1. Comparative values of Tolerance factor for $CsPbX_3$ PNCs

Compound	Tolerance factor
$CsPbI_3$ PNCs	0.851
$CsPbBr_3$ PNCs	0.862
$CsPbCl_3$ PNCs	0.870

S3. To determine the number of crystallites contained within a single PNC

Consider the side length of crystallite 'a' for $CsPbX_3$ PNCs

The volume V_1 of a crystallite is calculated using the formula: $V_1 = a^3$

The observed side length of PNCs from TEM are approximately double than crystallite size of $CsPbI_3$ and $CsPbBr_3$ PNCs

Where, $2a$ is the side length of the PNC.

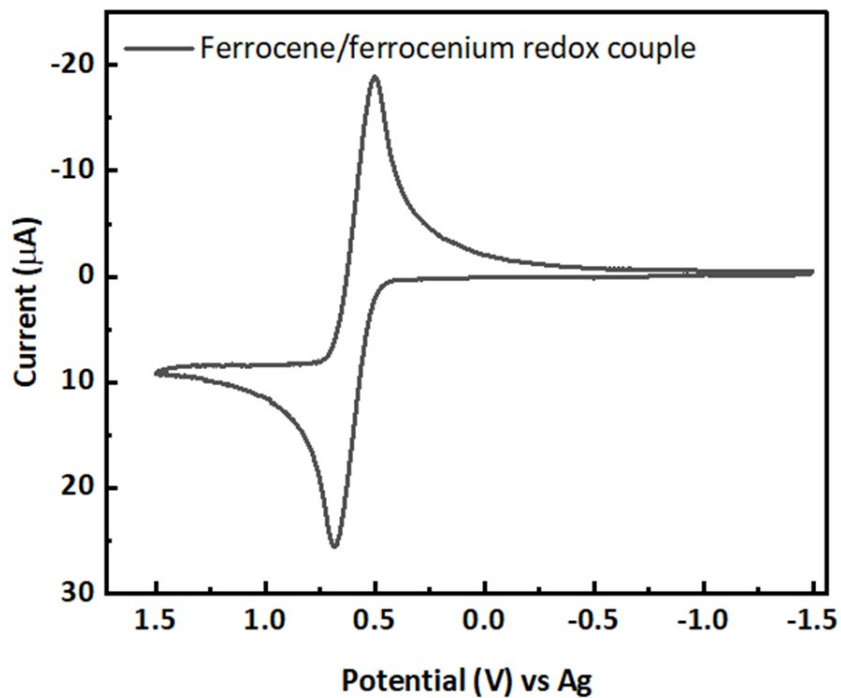The volume V_2 of a PNC is calculated using the formula: $V_2 = (2a)^3 = 8a^3$

The number of crystallites that can fit inside the single PNC can be calculated by dividing the volume of the single PNC by the volume of single crystallite:
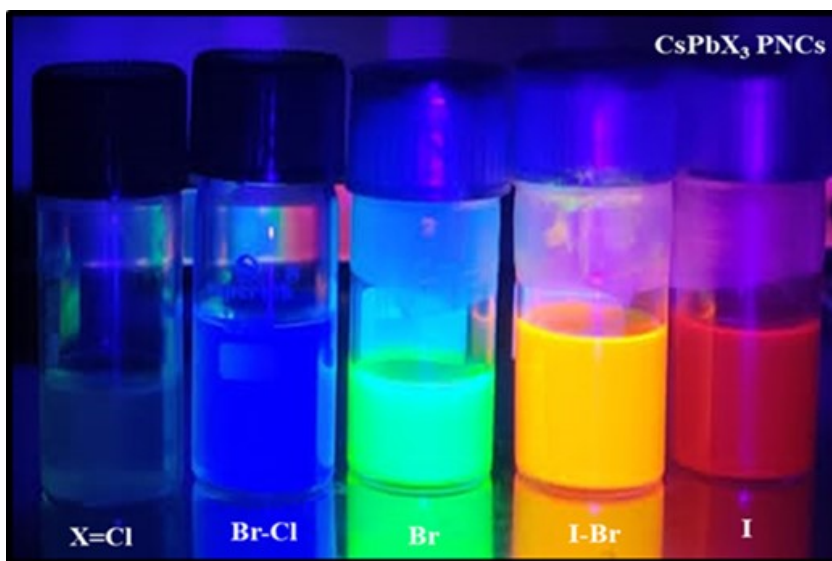
$$n = \frac{V_2}{V_1}$$

$$n = \frac{8a^3}{a^3}$$

$$n = 8$$

Hence, the single PNC of $CsPbI_3$ and $CsPbBr_3$ are made up of ~8 crystallites, suggesting his polycrystalline nature.

Figure S1. Cyclic voltammograms recorded for ferrocene/ferrocenium redox couple as internal standard in 50 mM TBAP solution in dichloromethane.


Figure S2. Digital photographs of colloidal $CsPbX_3$ (X = I, Br, Cl) PNCs dispersed in hexane under UV light.
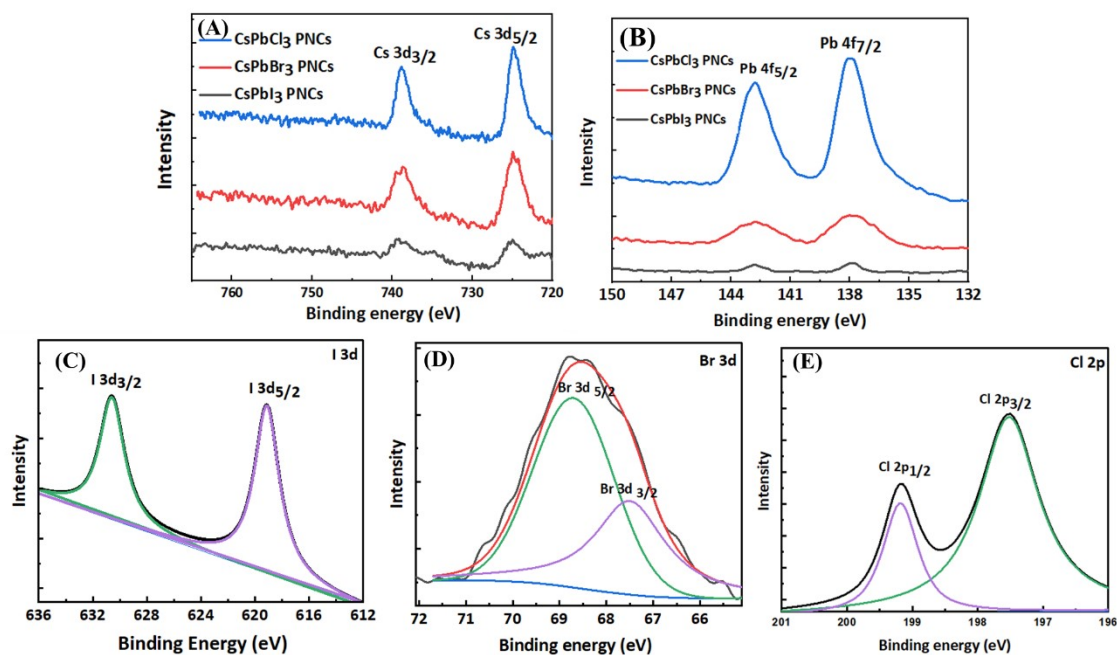
Figure S3. High-resolution XPS spectra of Cs, Pb and halogens. (A) Cs 3d and (B) Pb 4f spectra of CsPbX$_3$ PNCs. (C) I 3d, (D) Br 3d and (E) Cl 2p spectra of CsPbI$_3$, CsPbBr$_3$ and CsPbCl$_3$ PNCs.
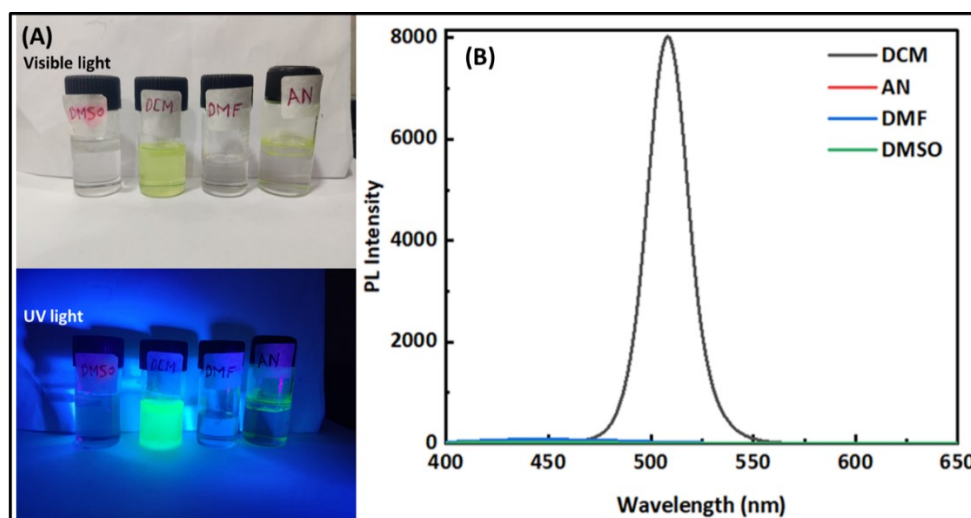
Figure S4. (A)Photographs CsPbBr$_3$ PNCs in different polar solvent [dimethyl sulfoxide (DMSO), dichloromethane (DCM), dimethylformamide (DMF), and acetonitrile (AN)] under visible light and under UV light; (B) Photoluminescence stability of CsPbBr$_3$ PNCs in different polar solvents.
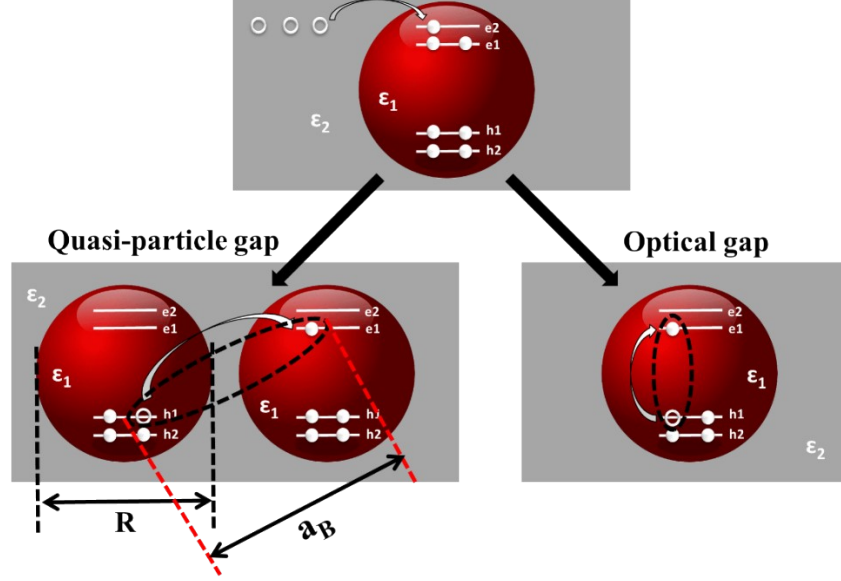
Figure S5. A) Loading of electrons into PNCs. B) The addition of one electron to one PNCs results in the simultaneous creation of a hole in another quantum dot, leading to the formation of a non-interacting electron-hole pair characterized by a quasi-particle gap (ε_{gap}^{qp}). C) The formation of an interacting electron-hole pair within a PNCs, induced by an exciton, gives rise to an optical band gap.

Consider a sphere of radius R and dielectric constant ε_2, surrounded by an organic entity here, oleic acid of dielectric constant ε_1.[39-41] In the initial stage, electron addition occurs to the neutral quantum dot of energy E_o. Consider the addition of 3 electrons whose arrangement will adhere to the Paulis exclusion principle. When one electron is added to the conduction level e1 of the quantum dot, a perturbation occurs followed by energy conservation as

$$E_1[e1] = E_0 + \varepsilon_{e1} \qquad (1)$$

Where, ε_{e1} is the electron quasiparticle energy which includes contribution from its own quantum confinement and polarization by its own image charge on the quantum dot surface. The energy required to add the first electron into the quantum dot is

$$\mu_1 = E_1[e_1] - E_0 \qquad (2)$$

Similarly, the energy of the quantum dot when a second electron is added into the conduction level e1 is

$$E_{e_1^2} = E_0 + 2\varepsilon_{e_1} + J_{e_1,e_1}$$

(3)

and the energy required to add this electron is $\mu_2 = E_2[e_1^2] - E_1[e_1]$

Now, the energy when the third electron is added into the conduction level e_2 of the quantum dot is

$$E_{[e_1^2 e_2^1]} = E_0 + 2\varepsilon_{e1} + J_{e_1 e_1} + 2J_{e_1 e_2} - K_{e_1 e_2}$$

(4)

Where, $K_{e_{1,e_2}}$ is exchange energy between parallel spin electrons in the two different conduction levels. Thus the energy required to add this electron is

$$\mu_3 = E_3[e_1^2 e_2^1] - E_2[e_1^2]$$

Next process is the creation of wannier exciton which is the bound state of an electron-hole pair arising due to coloumbic interaction between the charge carriers. The distance between the hole and electron in the Bohr radius of exciton a_B and is given by

$$a_B = \frac{4\pi\varepsilon_0\varepsilon_\infty\hbar^2}{e^2}\left(\frac{1}{m_e^*} + \frac{1}{m_h^*}\right)$$

(5)

Where, m_e^*, m_h^*, ε_o and ε_∞ are the effective electron, hole masses, dielectric constant of the quantum dot and medium respectively.

Using the Brus and Franceschetti model, the behavior of exciton occurs in two ways:

An electron can be removed from the valence band of one quantum dot to the conduction band of another quantum dot located at infinite distance from each other. This can be mathematically expressed as R $\ll a_B$, i.e., the electrons and holes have no limited bound states thereby deprived of any coloumbic interaction. This energy that is acquired to produce a non-interacting electron-hole pair is the quasi-particle energy and is modelled to a particle in a spherically symmetric potential well[2] with infinite barrier whose energy values can be expressed as,

$$E = E_g + E_{nl} = \varepsilon_g^{qp}$$

(6)

$$E_{nl} = \frac{\chi_{nl}^2\hbar^2}{2R^2}\left(\frac{1}{m_e^*} + \frac{1}{m_h^*}\right)$$

Where,

(7)

Where R is the nanocrystal radius and χ_{nl} are the roots of spherical Bessel function with n and l representing the principal and orbital quantum numbers respectively.

For the lowest state (n=, $l = 0$) $\chi_{n0} = \pi n$, energy can be expressed as

$$E_{nl} = \frac{\pi^2 \hbar^2}{2R^2} \left(\frac{1}{m_e^*} + \frac{1}{m_h^*} \right) \tag{8}$$

In contrast, an electron can be optically excited from the highest occupied valence band to the lowest unoccupied conduction band of the same quantum dot. This state occurs when R $\gg$ a_B, and now the electron and hole are limited to a space comparable with the exciton ground state in ideal infinite crystal and cannot be considered as a single particle but rather requires a Hamiltonian with two definite terms to define it; confinement and coloumbic potential.

$$H = -\frac{\hbar^2}{2m_e} \nabla_e^2 - \frac{\hbar^2}{2m_h} \nabla_h^2 - \frac{e^2}{\varepsilon |r_e - r_h|} + U(r) \tag{9}$$

Brus[3] had used a vibrational approach to solve this and this energy corresponding to the optical excitation energy is inclusive of the coloumbic interactions and is given by

$$E = E_g + \frac{\pi^2 \hbar^2}{2m_o R^2} \left(\frac{1}{m_e^*} + \frac{1}{m_h^*} \right) - \frac{Ae^2}{4\pi \varepsilon_o \varepsilon_\infty R} = \varepsilon_g^{op} \tag{10}$$

Where, e is the elementary charge, A is a coefficient equal to 1.786 for $1s_e 1s_h$ state.

Due to this electron-hole coloumbic interaction, the optical bandgap is lower than the actual quasiparticle band gap observed in cyclic voltammetry as proven above.
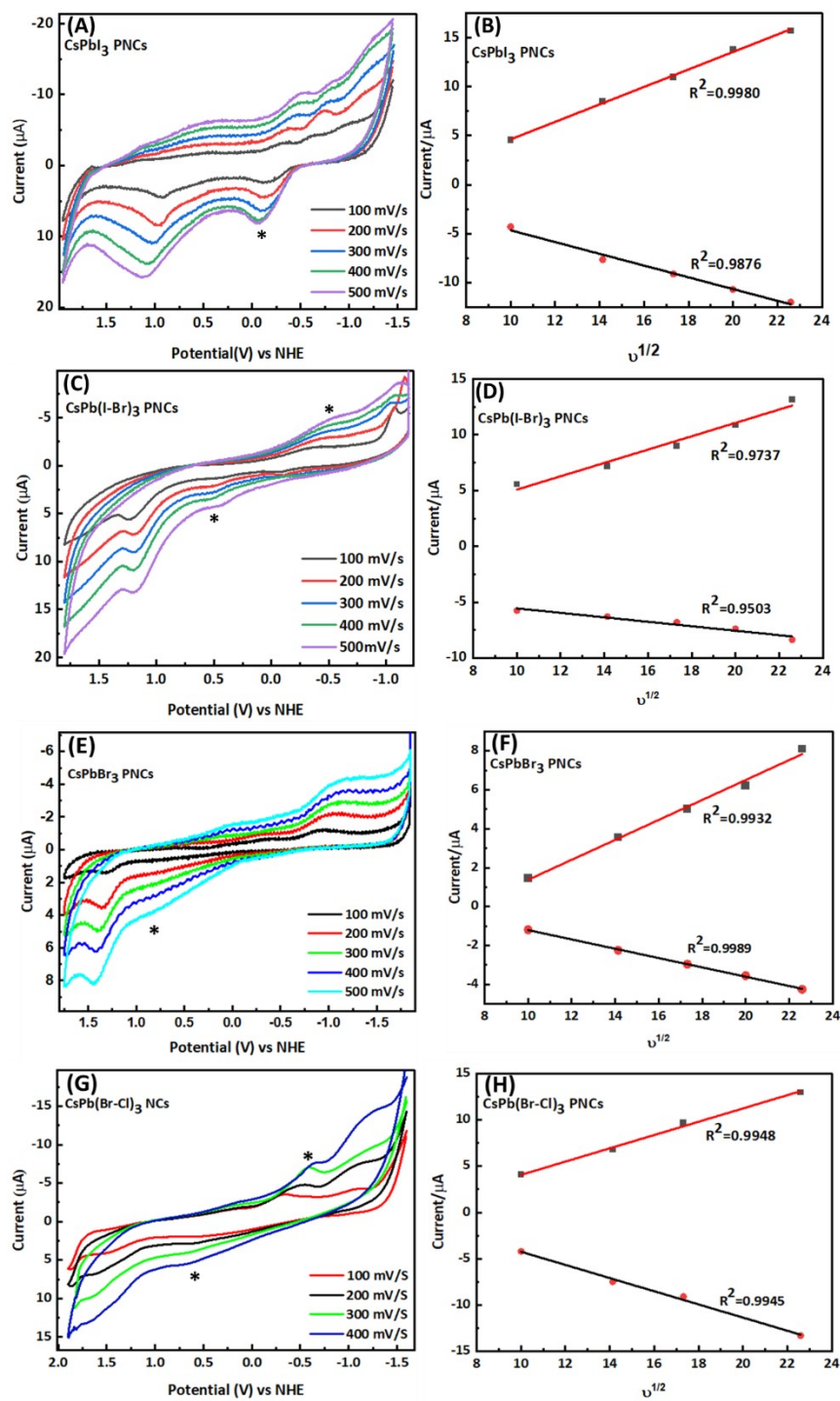
Figure S6. Scan-rate dependent response and linear fitting of peak currents of the CVs recorded on CsPbX$_3$ PNCs. (A-B)CsPbI$_3$; (C-D)CsPb(I-Br)$_3$; (E-F)CsPbBr$_3$; (G-H)CsPb(Br-Cl)$_3$.

Table S1. Comparative values of lattice parameter, microstrain, and dislocation density for CsPbX$_3$ PNCs

Sr.	2θ	FWHM	lattice parameter	Microstrain (10^{-3})	Dislocation density
A	**CsPbI$_3$ PNCs**				
1	14.16	0.8064	(100)	28.33	0.009299
2	20.48	2.5547	(110)	61.69	0.09183
3	28.77	1.0007	(200)	17.02	0.01364
4	35.37	1.2131	(211)	16.60	0.01939
5	42.84	2.9501	(220)	32.81	0.07631
B	**CsPb(I-Br)$_3$ PNCs**				
1	14.923	0.62411	(100)	20.79	0.00556
2	21.229	0.62344	(110)	14.51	0.00545
3	26.099	0.54215	(111)	10.21	0.00405
4	30.266	0.65924	(200)	10.64	0.00588
5	33.903	0.60717	(210)	8.69	0.00489
6	37.301	0.61666	(211)	7.97	0.00495
7	43.337	0.69968	(220)	7.68	0.00614
C	**CsPbBr$_3$ PNCs**				
1	14.965	1.17269	(100)	38.90	0.0196
2	21.24	0.94004	(110)	21.88	0.0126
3	30.35	0.90053	(200)	23.61	0.0291
4	37.54	1.10066	(211)	14.13	0.0158
5	43.64	1.12176	(220)	12.22	0.0157
D	**CsPb(Br-Cl)$_3$ PNCs**				
1	15.479	1.3167	(100)	42.27	0.0247
2	21.869	1.4618	(110)	33.02	0.0299
3	31.243	1.0439	(200)	16.29	0.0146
4	38.617	1.7185	(211)	21.40	0.0381
5	44.875	1.2887	(220)	13.62	0.0205
E	**CsPbCl$_3$ PNCs**				
1	15.565	1.0935	(100)	34.91	0.0169
2	22.792	4.2214	(110)	91.38	0.2475
3	31.639	1.2339	(200)	19.00	0.0204